High-Speed $In_{0.52}Al_{0.48}As$ Based Avalanche Photodiode With Top-Illuminated Design for 100 Gb/s ER-4 System

Song-Lin Wu, Naseem, Jhih-Min Wun, Rui-Lin Chao, Jack Jia-Sheng Huang, N.-W. Wang, Yu-Heng Jan, H.-S. Chen, C.-J. Ni, Hsiang-Szu Chang, Emin Chou, and Jin-Wei Shi, *Senior Member, IEEE*

***Abstract*—High-speed top-illuminated avalanche photodiodes (APDs) with large diameters (25 μm) are demonstrated for the application of 4-channels 100 Gb/s data rate. They achieve a bandwidth of 17 GHz at low-gain (M_G = 6.2; 3.6 A/W) and large-gain bandwidth (responsivity bandwidth) product (410 GHz (237.8 GHz-A/W); 55% external efficiency at the unit gain) while maintaining invariant high speed (14 GHz) under high power (0.5 mW) and 0.9 V_{br} operations. By packaging the demonstrated APD with a 25 Gb/s transimpedance amplifier in a 100 Gb/s ROSA package, a good sensitivity of around –20.6 dBm optical modulation amplitude (OMA) at the data rate of 25.78 Gb/s has been successfully demonstrated. The achieved sensitivity not only meets the required receiver sensitivity (–18.5 dBm OMA) in 100 GbE-ER-4 Lite (40 km) system, it is also comparable with that of the high-performance 100 Gb/s ROSA incorporated with the backside illuminated APD design. Overall, our novel APD structure can eliminate the costly flip-chip bonding package in the 100 Gb/s ROSA without sacrificing its sensitivity performance.**

***Index Terms*—Avalanche photodiode, photodiode.**

I. Introduction

HIGH-SENSITIVITY avalanche photodiodes (APDs) for >25 Gbit/sec operations at optical wavelength of 1.31 to 1.55 μm are key components for photodetection over 40–80 km fiber in 100 and 400 Gbit/sec ER-4 systems [1]–[3]. The APDs consisting of $In_{0.52}Al_{0.48}As$-based multiplication (M-) layer have attracted significant attention for 10 Gb/s and 25 Gb/s applications [4] due to their large gain-bandwidth product, high temperature stability, and reasonably low dark current characteristics at 1.31–1.55 μm wavelengths. In order to boost the gain-bandwidth product of these APDs for >25 Gb/s operation, a thin absorption (<1 μm) and multiplication (M-) layers (<100 nm) with a small diameter of active mesa (<20 μm) are usually necessary [1]–[4], which would degrade the unit-gain responsivity and result in a small optical alignment tolerance. The backside illuminated package [1], [2] is one of the possible solutions for enhancing the responsivity in these fast APDs because the topmost metal contact can serve as the reflector to fold the optical path of launched signal and enhance the photo-absorption process. However, as compared to the top-illuminated structure, this approach would significantly increase the packaging cost. In addition, to attain the desired operation gain, a high electric-field (>900 kV/cm) in the thin (<100 nm) M-layer is needed. This may lead to the occurrences of edge-breakdown in these APDs [1]. Recently, an inverted $In_{0.52}Al_{0.48}As$-based (N-side up) APD has been demonstrated [1] to enhance the lateral field confinement and suppress edge breakdown in the thin M-layer (<100 nm) for >25 Gbit/sec operation at 1.31 μm wavelength. Nevertheless, surface breakdown has become an issue for the inverted structure since the $In_{0.52}Al_{0.48}As$ M-layer is placed near the top surface. In addition, the large active mesa with $In_{0.53}Ga_{0.47}As$ absorption layer at the bottom may also cause a concern in the backside optical alignment process [1], [2], [5]. Besides the $In_{0.52}Al_{0.48}As$-based APDs, germanium-silicon (Ge-Si) based top-illuminated APDs is an alternative solution, which shows excellent sensitivity and speed at 1.31 μm wavelength [3]. However, an additional heater is usually installed in the package, in order to compensate the roll-off of Ge absorption layer at long wavelength side (>1.53 μm). The heater component would increase the overall cost of receiver module [3]. In this paper, we propose a novel N-side down APD with the $In_{0.52}Al_{0.48}As$ M-layer buried at the bottom side of device for 1.31 to 1.55 μm applications to circumvent the above-mentioned design challenges. Compared with the traditional N-side down $In_{0.52}Al_{0.48}As$-based APDs [6], our new device structure incorporates one additional charge layer above the M-layer in order to minimize the edge breakdown around the periphery of mesa and to reduce the dark current [7].

Manuscript received August 9, 2018; revised September 29, 2018; accepted October 11, 2018. Date of publication October 15, 2018; date of current version November 2, 2018. This work was supported in part by the Ministry of Science and Technology in Taiwan under Grant 105-2622-E-008-014-CC2 and in part by the Asian Office of Aerospace Research and Development under Grant FA2386-17-1-0033. *(Corresponding author: Jin-Wei Shi.)*

S.-L. Wu, Naseem, J.-M. Wun, and J.-W. Shi are with the Department of Electrical Engineering, National Central University, Taoyuan City 320, Taiwan (e-mail: qazwsx830719@gmail.com; naseem154148@st.jmi.ac.in; p3984011@hotmail.com; jwshi@ee.ncu.edu.tw).

R.-L. Chao is with the Department of Electrical Engineering, National Central University, Taoyuan City 320, Taiwan, and also with the Department of Photonics, National Chiao-Tung University, Hsinchu 300, Taiwan (e-mail: obscurotation.eo03g@g2.nctu.edu.tw).

J. J.-S. Huang and Y.-H. Jan are with the Source Photonics, West Hills, CA 91304 USA, and also with Source Photonics, Hsinchu 30844, Taiwan (e-mail: jack.huang@sourcephotonics.com; yuheng.jan@sourcephotonics.com).

N.-W. Wang, H.-S. Chen, C.-J. Ni, H.-S. Chang, and E. Chou are with Source Photonics, Hsinchu 30844, Taiwan (e-mail: nienwen.wang@sourcephotonics.com; hs.chen@sourcephotonics.com; cj.ni@sourcephotonics.com; hsiangszu.chang@sourcephotonics.com; emin.chou@sourcephotonics.com).

Color versions of one or more of the figures in this paper are available online at http://ieeexplore.ieee.org.

Digital Object Identifier 10.1109/JLT.2018.2876168

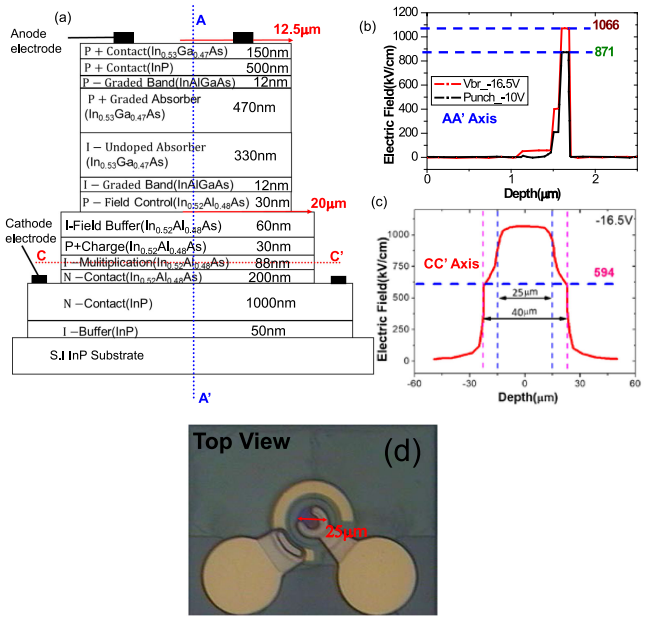

Fig. 1. (a) Conceptual cross-sectional view of the demonstrated device. The radius of active mesa is 12.5 μm as specified in this figure. The simulated E-field distributions in (b) vertical (A-A′) and (c) horizontal directions (C-C′). (d) Photo of top-view of the fabricated devices.

Furthermore, as compared to our previous work [7], the epi-layer structure in this newly demonstrated device has been further optimized to avoid the problem of absorption layer breakdown [8] and this leads to a significant improvement in gain-bandwidth product (161 [7] to 410 GHz). In addition, the demonstrated device is based on a simple top-illuminated structure without using costly flip-chip bonding [2] or backside illumination [1] packages. It has a large active mesa diameter of 25 μm for easy optical alignment from the top-side. At 1.31 μm wavelength, a good 3-dB O-E bandwidth (17 GHz) under low-gain operations ($M_G = 6.2$; 3.6 A/W) and a large gain-bandwidth product as high as 410 GHz with a 55% unit gain external efficiency can be simultaneously achieved. Furthermore, it can sustain a 3-dB bandwidth of around 14 GHz over a wide range of optical power (-19 to -3 dBm) under a moderate gain ($M_G = \sim 10$) operation. By packaging the demonstrated APD with a 25 Gbit/sec trans-impedance amplifier (TIA) in the 100 Gbit/sec ROSA, a good sensitivity (BER value of) as -20.6 dBm optical modulation amplitude (OMA) at 25.78 Gbit/sec data rate and pseudo randomness binary sequence (PRBS) length $2^{31} - 1$, has been successfully demonstrated. Such performance not only satisfies the required receiver sensitivity (-18.5 dBm OMA) for 100 GbE ER-4 Lite system in 40 km optical link [9], it is also comparable with the high-performance ROSAs with backside illuminated APDs designs [1], [2].

II. Design of Device Structure and Fabrication

Figures 1(a) shows the conceptual cross-sectional views of the demonstrated top-illuminated device structure, not drawn in scale for simplicity. From top to bottom, it is composed of the p^+-$In_{0.53}Ga_{0.47}As$ contact layer, p^+-InP window layer, p-type partially depleted $In_{0.53}Ga_{0.47}As$ absorber, two p-type $In_{0.52}Al_{0.48}As$ charge layers, one intrinsic $In_{0.52}Al_{0.48}As$ field buffer layer, one intrinsic $In_{0.52}Al_{0.48}As$ M-layer, and N^+ $In_{0.52}Al_{0.48}As$ /InP contact layers. Here, the partially depleted p-type absorber, which has a graded doping profile (top: to bottom:) is used to shorten the hole transit time, accelerate the electron diffusion process, and increase the high-power and linearity performances of our APD [1], [10]. Here, the total thickness of $In_{0.53}Ga_{0.47}As$ absorber is 0.8 μm and the ratio of depleted versus p-doped region is chosen to balance the RC delay and internal carrier transit/avalanche-delay time under low gain operation ($M_G < 5$) [7]. In order to shorten the avalanche delay time, a thin M-layer (around 90 nm) is chosen in our device structure [1], [4]. The detail of our epi-layer structure can be referred to our previous work [7]. As shown in Fig. 1(a), there is a triple mesa structure with different diameters in our device. The first mesa with a 25 μm diameter, is etched through the upper charge (field-control) layer and stop at the 60 nm $In_{0.52}Al_{0.48}As$ buffer layer. The additional charge layer in the upper mesa is expected to effectively confine the strong E-field at the bottom M-layer within the range of 25 μm diameter. Compared with our previous work [7], the doping density in those two charge layers have been further optimized to avoid the problem of absorption layer breakdown [7], [8], which limits the gain-bandwidth product of APD. Fig. 1(b) and (c) shows the simulated E-field distributions in vertical and horizontal directions of our device at around breakdown voltage (V_{br}: -16.5 V), respectively. As shown in Fig. 1(b), we can clearly see that even operated under V_{br}, the E-field in the $In_{0.53}Ga_{0.47}As$ absorption layer (<100 kV/cm) is still much lower than it's critical filed (~150 kV/cm [7]). Furthermore, as shown in Fig. 1(c), we can clearly see that the horizontal E-field in the M-layer is well confined in the range of 25 μm diameter (1000 kV/cm), and it can be greatly reduced to around 590 kV/cm at the edge of second mesa to suppress the edge breakdown in our device. Fig. 1(d) shows the top-view of fabricated device with a 25 μm diameter of active mesa. The mask defined diameter of optical window is 16 μm.

III. Measurement Results

Figure 2 shows the measured bias-dependent dark current and photocurrent of device subjected to different optical pumping power at optical wavelength of 1.31 μm. The breakdown voltage (V_{br}) was at around -16.5 V and the corresponding dark current and operational gain at 0.9 V_{br} was around 470 nA and 14.8, respectively. During our measurement, we assumed a zero coupling loss from injected light into our active device. With a 0.8 μm-thick $In_{0.53}Ga_{0.47}As$ absorption layer, the theoretical maximum unit gain responsivity is around 0.58 A/W at 1.31 μm wavelength. The value of unit gain shown here should represent an underestimation of the real operation gain of our device. We can clearly see that there are two punch-through voltages (V_{pt}: -9.6 and -12 V) in the measured traces of photocurrent versus reverse bias voltages. These two V_{pt} correspond to the two different charge layers in our epi-layer structure as discussed. The measured responsivity at first V_{pt} (-9.6 V) is around 0.53 A/W, which corresponds to the operation gain (M_G)

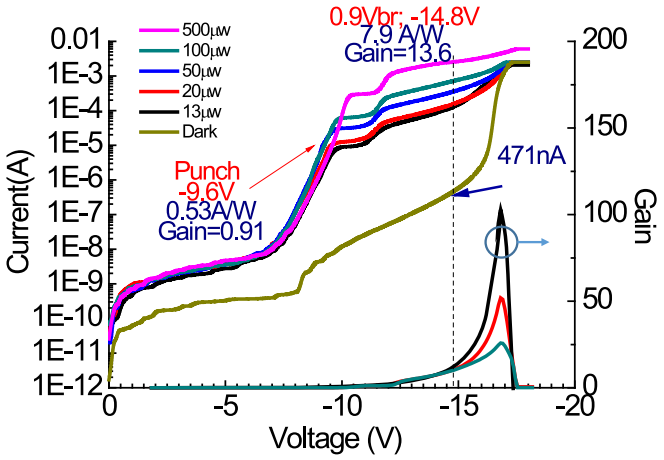

Fig. 2. The measured dark current and photocurrent versus bias voltages under different optical pumping power at 1.31 μm wavelength.

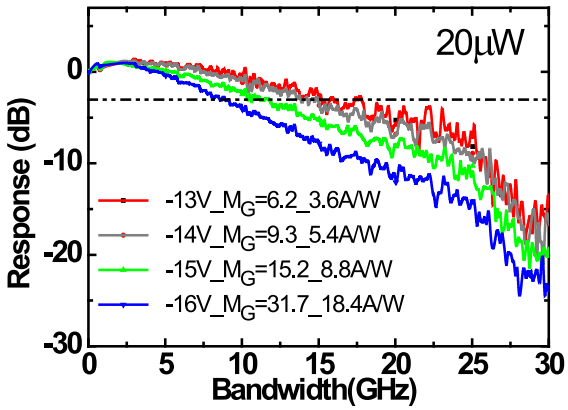

Fig. 3. The measured bias dependent O-E frequency responses under 20 μW optical pumping power at 1.31 μm wavelength.

of around 0.91. The gain versus bias voltages of our device under three different optical pumping power (13, 20, and 100 μW) are also provided in this figure for reference. As can be seen, all the measured operation gains significantly reduce when the reverse bias voltage is over V_{br} due to the tremendous increase of dark current, which occupies most part of the measured total current (i.e., summation of photocurrent and dark current). In addition, we can clearly see that the maximum operation gain gradually decreases with increasing pumping power. This phenomenon can be explained by the space charge screening effect induced by the photo-generated holes in the undoped $In_{0.53}Ga_{0.47}As$ absorption layer, which reduce the net E-field and multiplication gain in the M-layer [11].

Figures 3 and 4 show the measured bias-dependent O-E frequency responses of the top-illuminated APD device under low (20 μW) and high (0.5 mW) optical pumping power at 1.31 μm wavelength, respectively. Under low optical pumping power (20 μW) and low operation gain ($M_G = 6.2$; 3.6 A/W at -13 V), the measured 3-dB O-E bandwidth is around 17 GHz. On the other hand, when the optical pumping power reaches 0.5 mW, an invariant 3-dB O-E bandwidth as 14 GHz can still be sustained from low to high operation gains (bias voltages). Such

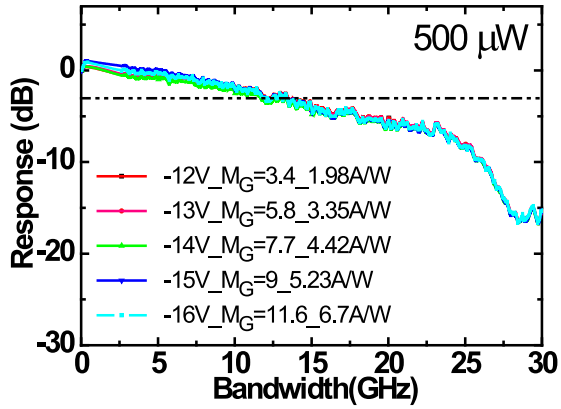

Fig. 4. The measured bias dependent O-E frequency responses under 0.5 mW optical pumping power at 1.31 μm wavelength.

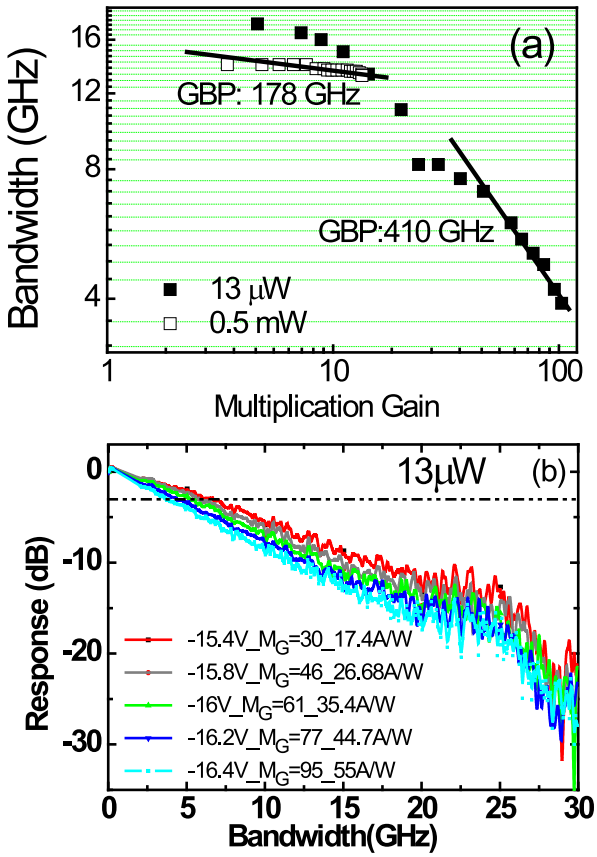

Fig. 5. (a) The measured 3-dB O-E bandwidths versus multiplication gain at low (13 μW) and high (0.5 mW) optical pumping powers. (b) The measured O-E frequency responses under low power (13 μW) and high gain operations.

high-speed and high-linearity performances are comparable with the reported data from $In_{0.52}Al_{0.48}As$-based APD with a smaller active diameter (20 vs. 25 μm) and back-side illumination package (17 GHz 3-dB O-E bandwidth at 9.1 A/W) [11], [12].

Figure 5(a) shows the measured 3-dB O-E bandwidths versus operation gains of our device under low (13 μW) and high (0.5 mW) optical pumping powers. As can be seen, for the case

of low pumping power, a gain-bandwidth (GB) product as high as 410 GHz with a 55% unit-gain external efficiency can be achieved in our demonstrated device. On the other hand, the values of GB product gradually decreases to 178 GHz when the optical pumping power reaches 0.5 mW, which can be attributed to due to the reduction in multiplication gain versus the increase of optical power as discussed in Fig. 2. Fig. 5(b) shows the corresponding measured O-E responses under high-gain and low-power (13 μW) operation. As compared to our previous work [7], there is a significant improvement in GB product (410 vs. 161 GHz) likely due to the effective suppression of the absorption layer breakdown in our new design of charge layer [7], [8]. The achieved GB (410 GHz) and corresponding bandwidth-responsivity products $(237.8\,\mathrm{GHz} \times \mathrm{A/W})$ is even better than that of the reported high-performance Ge-Si APDs (340 GHz) [13] and the waveguide-type (320 GHz) [14] and backside-illuminated $214\,\mathrm{GHz} \times \mathrm{A/W}$ [12] $In_{0.52}Al_{0.48}As$-based APDs with a similar (~90 nm) [12] or larger (~150 nm) M-layer thickness [14]. The achieved high GB product (410 GHz) can be attributed to the aggressive downscaling of our M-layer thickness (~90 nm) and significant dead space effect inside M-layer [15], [16]. Besides, such excellent performance in terms of GB product also implies that our dual charge layers design can effectively suppress the edge breakdown and allow the avalanche process concentrate at the small volume of M-layer below active mesa. Furthermore, the high GB product usually accompanies with a small excess noise and k-factor in APD [16]. As compared to the reported value of k-factor (~0.15) of $In_{0.52}Al_{0.48}As$ APD with the same M-layer thickness as 90 nm with ours [1], [12], our device is likely to have a smaller k-factor due to its larger GB product as discussed. In order to calculate and explain the large value of GB product and low excess noise in such kind of thin M-layer APD, the dead-space-multiplication theory (DSMT) has been developed [15], [16]. Further study in theoretical value of GB product, k-factor, and excess noise in our novel device structure is being investigated by use of DSMT.

In order to perform the sensitivity measurement of our APD chip, we integrated it with a 25 Gbit/sec transimpedance amplifier (TIA)[1] in a packaged ROSA module. The inset in Fig. 6 shows the picture of the packaged APD. During the measurement, we adopted a commercial 25 Gbit/sec electro-absorption modulated laser (EML)[2] to serve as the light source with a 4.8 dB extinction ratio (ER). The chosen ER was adjusted to maintain the averaged power to be the same as optical modulation amplitude (OMA). The date rate used for testing is 25.78 Gbit/sec with a pseudorandom binary sequence (PRBS) length as $2^{31} - 1$.

Figure 6 shows the measured BER values versus the OMA. The horizontal line here represents the required BER value (5×10^{-5}) to meet KR4 forward error correction (FEC) coding. The solid symbol represents the APD receiver module integrated with a clock and data recovery (CRD) unit, and the open symbol shows the BER from the same module without

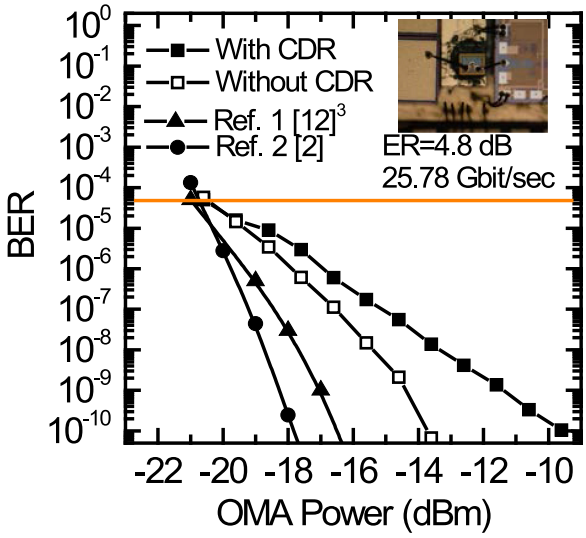

Fig. 6. The measured BER values vs. OMA of our receiver modules with/without CDR unit at 1.31 μm optical wavelength and 25.78 Gbit/sec data rate. The inset shows our home-made APD chip packaged in the ROSA module. The measured BER curves of two commercial available ROSAs [2], [12][3] were also given for references.

the CDR integration. Here, the measured BER curves based on two different commercially available backside-illuminated APD chips in ROSA package [2], [12][3] are also shown for comparisons. During BER testing, the bias voltage of each ROSA has been optimized for the highest sensitivity. For our devices, such bias voltage locates at around -15.5 V, which corresponds to ~9 A/W responsivity under 20 μW optical pumping power. The achieved sensitivity in all these three modules are very close (around -20.6 dBm OMA) and it can satisfy the specification for the application of 100 GbE-ER4-Lite (40 km) [9], which requires a receiver operated at 25 Gbit/sec and 1.31 μm optical wavelength with a -18.5 dBm OMA sensitivity under a BER value of 5×10^{-5}. Such result clearly indicates that our top-illuminated APD structure can effectively save the cost for 100 Gbit/sec APD ROSA package without sacrificing its sensitivity performance for ER-4 Lite application. Nevertheless, our device suffers worse error-free $(\mathrm{BER} < 1 \times 10^{-12})$ sensitivity performance than those of two reference backside-illuminated APDs [2], [12]. This may be attributed to our top-illuminated design that incorporates a larger diameter of active mesa (25 vs. <20 μm) and junction capacitance than those of backside-illuminated ones. Here, the extracted value of our device capacitance is close with the upper limit of input capacitance (100 fF) of our integrated TIA. In order to further improve the sensitivity performance of our ROSA module, an improved design of our APD with a smaller junction capacitance is necessary.

II. Conclusion

In conclusion, we demonstrate a novel APD structure with excellent performance for 100 GbE-ER-4 Lite application. By using a simple vertical-illuminated structure with a large active

[1]Semtech; 200 Flynn Road, Camarillo, CA 93012. Product: GN1085.

[2]Source Photonics; 8521 Fallbrook Avenue #200, West Hills, CA 91304 Product: SPQ-CE-LR-CDFB.

[3]NTT Electronics Corporation; 1-1-32 Shin-urashimacho, Kanagawa-ku, Yokohama-shi, Kanagawa, 221-0031, Japan. Product: 100G APD-ROSA.

mesa (25 μm), we can attain a high O-E bandwidth ($\sim$17 GHz) under a moderate gain ($M_G = 6.2$) with a large dynamic range (-20 to -3 dBm). By packaging the top-illuminated APD device with a 25 Gbit/sec TIA in a ROSA module, a good sensitivity as -20.6 dBm OMA can be achieved to meet the required specification of sensitivity for receiver in 100 GbE-ER-4 Lite system for 40 km transmission. Such sensitivity performance is comparable with that of commercially available ROSAs with backside-illuminated APDs inside under the same test conditions. Overall, our demonstrated APD with top-illuminated design can not only eliminate the costly flip-chip bonding package in the ROSA but also satisfy the required sensitivity for the 100 GbE-ER-4 Lite system.

REFERENCES

[1] M. Nada, Y. Yamada, and H. Matsuzaki, "Responsivity-bandwidth limit of avalanche photodiodes: Toward further ethernet systems," *IEEE J. Sel. Topics Quantum Electron.*, vol. 24, no. 2, Mar./Apr. 2018, Art. no. 3800811.

[2] Product: APD 16L on Submount, Albis Optoelectronics AG, Rueschlikon, Switzerland, 2014.

[3] M. Huang *et al.*, "Germanium on silicon avalanche photodiode," *IEEE J. Sel. Topics Quantum Electron.*, vol. 24, no. 2, Mar./Apr. 2018, Art. no. 3800911.

[4] J. C. Campbell *et al.*, "Recent advances in avalanche photodiodes," *IEEE J. Sel. Topics Quantum Electron.*, vol. 10, no. 4, pp. 777–787, Jul./Aug. 2004.

[5] M. Nada, Y. Muramoto, H. Yokoyama, T. Ishibashi, and H. Matsuzaki, "Triple-mesa avalanche photodiode with inverted P-down structure for reliability and stability," *J. Lightw. Technol.*, vol. 32, no. 8, pp. 1543–1548, Apr. 2014.

[6] E. Ishimura *et al.*, "Degradation mode analysis on highly reliable guarding-free planar InAlAs avalanche photodiodes," *J. Lightw. Technol.*, vol. 25, no. 12, pp. 3686–3693, Dec. 2007.

[7] Yi-Han Chen *et al.*, "Top-Illuminated $In_{0.52}Al_{0.48}As$-based avalanche photodiode with dual charge layers for high-speed and low dark current performances," *IEEE J. Sel. Topics Quantum Electron.*, vol. 24, no. 2, Mar./Apr. 2018, Art. no. 3800208.

[8] N. Duan *et al.*, "Detrimental effect of impact ionization in the absorption region on the frequency response and excess noise performance of InGaAs-InAlAs SACM avalanche photodiodes," *IEEE J. Quantum Electron.*, vol. 41, no. 4, pp. 568–572, Apr. 2005.

[9] 2010. [Online]. Available: http://www.ieee802.org/3/ba/

[10] J.-W. Shi and C.-W. Liu, "Design and analysis of separate-absorption-transport-charge-multiplication traveling-wave avalanche photodetectors," *J. Lightw. Technol.*, vol. 22, no. 6, pp. 1583–1590, Jun. 2004.

[11] M. Nada, Y. Muramoto, H. Yokoyama, and H. Matsuzaki, "High-speed high-power-tolerant avalanche photodiode for 100-Gb/s applications," in *Proc. IEEE Photon. Soc. Meeting,* San Diego, CA, USA, 2014, Paper TuA1.4.

[12] M. Nada, T. Yoshimatsu, Y. Muramoto, H. Yokoyama, and H. Matsuzaki, "Design and performance of high-speed avalanche photodiodes for 100-Gb/s systems and beyond," *J. Lightw. Technol.*, vol. 33, no. 5, pp. 984–990, Dec. 2015.

[13] Y. Kang *et al.*, "Monolithic germanium/silicon avalanche photodiodes with 340 GHz gain-bandwidth product," *Nature Photon.*, vol. 3, pp. 59–63, Dec. 2009.

[14] G. S. Kinsey, J. C. Campbell, and A. G. Dentai, "Waveguide avalanche photodiode operating at 1.55 μm with a gain-bandwidth product of 320 GHz," *IEEE Photon. Technol. Lett.*, vol. 13, no. 8, pp. 842–844, Aug. 2001.

[15] B. E. A. Saleh, M. M. Hayat, and M. C. Teich, "Effect of dead space on the excess noise factor and time response of avalanche photodiodes," *IEEE Trans. Electron Devices*, vol. 37, no. 9, pp. 1976–1984, Oct. 1990.

[16] M. A. Saleh *et al.*, "Impact-ionization and noise characteristics of thin III-V avalanche photodiodes," *IEEE Trans. Electron Devices*, vol. 48, no. 12, pp. 2722–2731, Dec. 2001.

Song-Lin Wu was born in Taipei, Taiwan, on July 19, 1994. He is currently working toward the Master's degree in solid state physics with the Department of Electrical Engineering, National Central University, Taoyuan City, Taiwan. His current research interests include high-speed and high-performance avalanche photodiode.

Naseem was born in Punjab, India, in 1991. He received the M.Tech. degree from the Department of Nanotechnology, Jamia Millia Islamia, New Delhi, India. He is currently working toward the Ph.D. degree with the Department of Electrical Engineering, National Central University, Taoyuan City, Taiwan. His current research interests include high-speed photodiodes and avalanche photodiode for optical receiver.

Jhih-Min Wun was born in Taoyuan City, Taiwan, on October 3, 1988. He is currently working toward the Ph.D. degree with the Department of Electrical Engineering, National Central University, Taoyuan City, Taiwan. His current research interests include high-speed optoelectronic device measurement and sub-THz high-speed photodiode.

Rui-Lin Chao was born in Taipei, Taiwan, on October 27, 1991. He received the B.S. degree under Undergraduate Honors Program of Nano Science and Engineering, Chiao Tung University, Hsinchu, Taiwan, in 2014. He is currently working toward the Ph.D. degree with the Department of Elecro-Optics, Chiao Tung University, under the guidance of advisor Prof. Jyehong Chen and also under the guidance of co-advisor Prof. Jin-Wei Shi, National Central University, Taoyuan City, Taiwan, focusing on slow light high-speed silicon based modulator, high-speed photodetector, and high-speed laser development and design.

Jack Jia-Sheng Huang received the B.S. degree in physics from National Taiwan University, Taipei, Taiwan, in 1992, and the M.S. and Ph.D. degrees in materials science from the University of California, Los Angeles, Los Angeles, CA, USA, in 1996 and 1997, respectively. During 1992–1993, he was a Research Assistant with the Institute of Atomic and Molecular Sciences, Academia Sinica, Taipei, Taiwan, studying surface physics of gallium ion beam in ultra-high vacuum. From 2000 to 2015, he was a Wafer Fab R&D/Operations Manager with Emcore, Alhambra, CA, USA, working on device design/process/characterization, reliability, electrostatic discharge, and failure analysis of analog BH lasers and digital ridge lasers for cooled and uncooled applications. He is currently a Senior R&D Scientist/Manager with Source Photonics, West Hills, CA, USA, working on advanced photonics devices including 100G DML, 40G CWDM DFB, 10G DFB, and 10G FP lasers as well as 10G and 25G APD photodetectors. His R&D projects also inlcude device reliability physics and device characterization. He has authored or coauthored more than 90 publications in international journals and conferences in the areas of optoelectronics and ICs and holds 6 U.S. patents and 1 U.K. patent. From 1997 to 2000, he was a member of the Technical Staff, Lucent Technologies, Bell Labs, Orlando, FL, USA, working on electromigration, stress migration, and failure analysis of 0.3, 0.25, 0.2, and 0.16 mm ASIC and FPGA devices using CMOS technology.

Nienwen Wang received the B.S. degree from National United University. He is working at Source Photonics Inc., as Sr. Engineer of Advanced OSA.

Yu-Heng Jan was born in Taipei, Taiwan, on November 6, 1965. He received the Ph.D. degree in electrical and computer engineering from the University of California, Santa Barbara, Santa Barbara, CA, USA, in 1997. In 1997, he joined the Optical Division, MRV Communications, Chatsworth, CA, USA, where he focused on the design and manufacturing of CWDM DFB lasers and systems. In 2007, he became a COO and a General Manager with Source Photonics, Hsinchu, Taiwan, where he managed operations and R&D activities. He is currently a Chief Device Officer with Source Photonics, where he focuses on high-speed devices for data center and PON applications.

H.-S. Chen received the Ph.D. degree with the Graduate Institute of Photonics and Optoelectronics, National Taiwan University, Taipei, Taiwan, in 2006. Since June 2007, he has been a Postdoctoral Research Fellow with the Institute of Physics, Acadmia Sinica, Taipei, Taiwan. From 2011 to 2013, he was a Postdoctoral Fellow with the Institute of Photonics and Optoelectronics, National Taiwan University. In 2014, he joined Source Photonics, Hsinchu, Taiwan, as a Manager of Advanced Process Development. His research interests include surface plasmon, near field optics, ultrafast laser, nanorod array LED, and optical sensors.

C.-J. Ni received the B.S. degree in chemical engineering from National Chung Cheng University, Chiayi, Taiwan, in 2006, and the M.S. and Ph.D. degrees in chemical engineering from National Cheng Kung University, Tainan, Taiwan, in 2008 and 2014, respectively. He is currently an R&D engineer with the Division of Advanced Process Development, Source Photonics, Hsinchu, Taiwan.

Hsiang-Szu Chang received the M.S. and Ph.D. degrees from the Solid-State Optics Lab, Department of Physics, National Central University, Taoyuan City, Taiwan, in 2002 and 2009, respectively. He is currently a Senior Engineer of Product Development, OE device, with Source Photonics, Hsinchu, Taiwan.

Emin Chou received the B.S. degree in nuclear engineering from National Tsing Hua University, Hsinchu, Taiwan, in 1997, and the M.S. degree with the MBE Lab, Department of Electronics Engineering, National Chiao Tung University, Hsinchu, Taiwan, in 1999. He is currently the Senior Director of Product Development, Advanced OSA and OE Devices, with Source Photonics, Hsinchu, Taiwan.

Jin-Wei Shi (M'03–SM'12) was born in Kaohsiung, Taiwan, on January 22, 1976. In 2003, he joined the Department of Electrical Engineering, National Central University, Taoyuan City, Taiwan, where he has been a Professor since 2011. During 2011–2012 and 2016–2017, he joined the Department of Electrical and Computer Engineering, University of California, Santa Barbara, Santa Barbara, CA, USA, as a Visiting Professor. He has authored or coauthored more than 4 book chapters, 140 journal papers, and 200 conference papers and holds 30 patents. His current research interests include ultra-high speed/power photodetectors, electro-absorption modulator, THz photonic transmitter, and VCSELs. He was the recipient of the 2010 Da-You Wu Memorial Award.